VOLUME 6, NUMBER 1, JANUARY 2006

NANO LETTERS

Letters

Quantum Dots with a Paramagnetic Coating as a Bimodal Molecular Imaging Probe

Willem J. M. Mulder,*,† Rolf Koole,‡ Ricardo J. Brandwijk,§ Gert Storm,|| Patrick T. K. Chin,⊥ Gustav J. Strijkers,† Celso de Mello Donegá,‡ Klaas Nicolay,† and Arjan W. Griffioen§

Biomedical NMR, Department of Biomedical Engineering, Eindhoven University of Technology, P.O. Box 513, 5600 MB Eindhoven, The Netherlands, Debye Institute, Condensed Matter and Interfaces, Utrecht University, P.O. Box 80.000, 3508 TA Utrecht, The Netherlands, Angiogenesis Laboratory, Research Institute for Growth and Development, Department of Pathology/Internal Medicine, Maastricht University & University Hospital, P.O. Box 5800, 6202 AZ Maastricht, The Netherlands, Department of Pharmaceutics, Utrecht Institute for Pharmaceutical Sciences (UIPS), 3508 TB, Utrecht, The Netherlands, and Laboratory of Macromolecular and Organic Chemistry, Eindhoven University of Technology, P.O. Box 513, 5600 MB Eindhoven, The Netherlands

Received September 29, 2005; Revised Manuscript Received November 9, 2005

ABSTRACT

MRI detectable and targeted quantum dots were developed. To that aim, quantum dots were coated with paramagnetic and pegylated lipids, which resulted in a relaxivity, r_1, of nearly 2000 $mM^{-1}s^{-1}$ per quantum dot. The quantum dots were functionalized by covalently linking $\alpha v\beta 3$-specific RGD peptides, and the specificity was assessed and confirmed on cultured endothelial cells. The bimodal character, the high relaxivity, and the specificity of this nanoparticulate probe make it an excellent contrast agent for molecular imaging purposes.

A rapidly growing field in experimental diagnostic radiology is molecular imaging, aiming to image biological processes in vivo and noninvasively at the cellular and molecular level.[1] Magnetic resonance imaging (MRI) has become one of the most important imaging modalities in both clinical and research settings[2] because of its fast scan times, its capacity to produce excellent quality and high-resolution images, and because there is no need for radiochemicals. The MRI signal arises from the excitation of the magnetic moments of hydrogen nuclei of mainly water and lipids, placed in a strong magnetic field. MR images are known for their excellent soft tissue contrast. The most important contrast mechanisms are based on differences in the transverse (T_2) and longitu-

* Corresponding author. E-mail: w.j.m.mulder@tue.nl. Phone: +31 40 2474853. Fax: +31 40 2432598.

† Biomedical NMR, Department of Biomedical Engineering, Eindhoven University of Technology.

‡ Debye Institute, Condensed Matter and Interfaces, Utrecht University.

§ Angiogenesis Laboratory, Research Institute for Growth and Development, Department of Pathology/Internal Medicine, Maastricht University & University Hospital.

|| Department of Pharmaceutics, Utrecht Institute for Pharmaceutical Sciences (UIPS).

⊥ Laboratory of Macromolecular and Organic Chemistry, Eindhoven University of Technology.

10.1021/nl051935m CCC: $33.50
Published on Web 11/24/2005

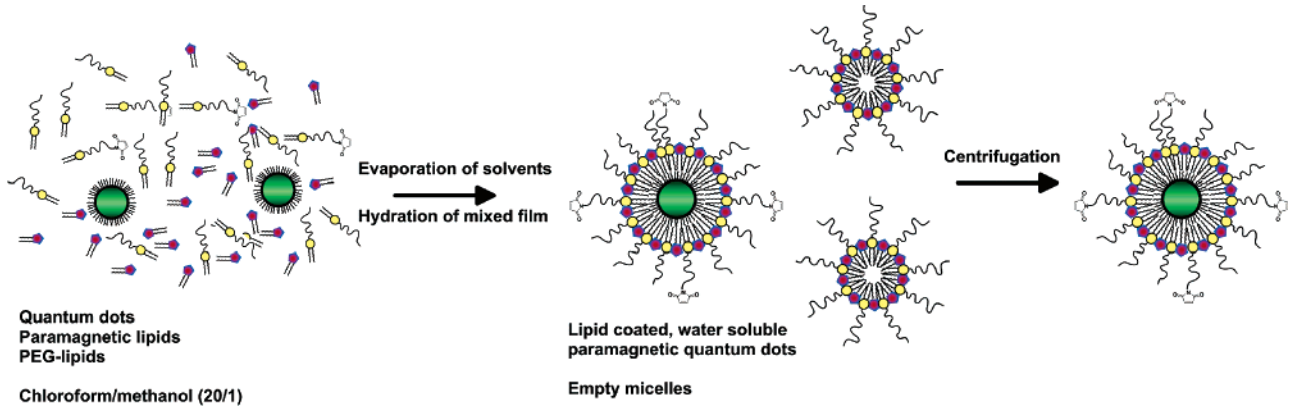

Figure 1. Schematic representation of the preparation of QDs with a paramagnetic micellular coating.

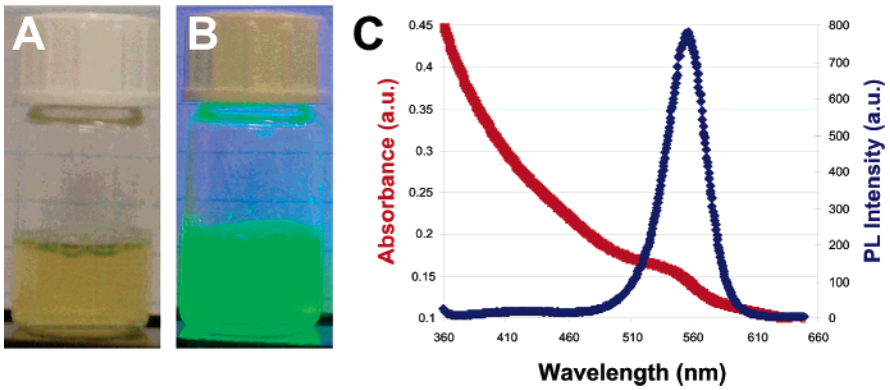

Figure 2. Optical properties of pQDs in HEPES buffer. (A) Under weak daylight illumination; (B) photoluminescence under 365-nm excitation; (C) UV−vis absorption (red) and PL (blue) spectra.

dinal (T_1) relaxation times. These relaxation times can be manipulated by the use of paramagnetic contrast agents, for example, Gd-DTPA, which efficiently shorten T_1 and therefore give rise to signal enhancement in T_1-weighted images.[3] The introduction of MRI as a molecular imaging modality has been hampered by its low sensitivity compared to nuclear methods such as PET and SPECT.[4] With recent developments in chemistry and the synthesis of powerful, innovative,[4] specific, and multimodal contrast agents, for example, by introducing fluorescent properties as well,[5−7] MRI is becoming increasingly important for molecular imaging. Quantum dots, semiconductor nanocrystals in a size range of 2−6 nm, have gained much interest in the past few years for biological imaging purposes,[8] especially because of their bright fluorescence, their photostability, and their narrow and tunable emission spectrum. The in vivo use requires the quantum dots to be water-soluble and biocompatible.[9] Efforts have been undertaken to achieve these goals, and quantum dots have been used successfully for imaging studies of live cells[9−11] and animal models,[12−14] mainly in combination with two-photon fluorescence microscopy.

Here we report on the synthesis of pegylated and paramagnetic quantum dots (pQDs) with a high relaxivity, r_1, which make them detectable by both MRI and fluorescence microscopy. Angiogenesis, the formation of new blood vessels, occurs in many pathophysiological processes, and the in vivo imaging of this process is therefore of considerable biomedical interest. Specificity for angiogenic blood vessels was introduced by conjugating the pQDs with cyclic RGD peptides. The arginine-glycine-aspartic acid (RGD) peptide sequence is present in many extracellular matrix proteins[15] and is recognized by $\alpha v\beta 5$- and $\alpha v\beta 3$-integrins,[16] of which the latter is overexpressed on both the surface of angiogenic endothelial cells and tumor cells.[17−19] The contrast agent was characterized in terms of relaxation and optical properties and was tested in vitro on cultured human umbilical vein endothelial cells (HUVEC).

High-quality CdSe/ZnS core/shell QDs were synthesized by injection of precursors ($Cd(acetate)_2$ and Se in trioctylphosphine) into a hot coordinating solvent mixture (trioctylphosphineoxide/hexadecylamine; TOPO/HDA) following methods reported in the literature,[20] with some adaptations (a detailed description can be found in the Supporting Information). A micellular and paramagnetic coating was applied to the QDs in order to make them MR-detectable, water-soluble, and biocompatible.[9,21] This micellular coating was composed of a pegylated phospholipid, PEG-DSPE (1,2-distearoyl-sn-glycero-3-phosphoethanolamine-*N*-[methoxy-(poly(ethylene glycol))-2000]), and a paramagnetic lipid, Gd-DTPA-BSA (Gd-DTPA-bis(stearylamide). PEG-lipids are used commonly to stabilize liposomes for pharmaceutical applications because the PEG chains form a hydrophilic coating at the liposomal surface. This results in enhanced circulation half-lives in vivo because pegylated liposomes are protected from interactions with plasma proteins and are

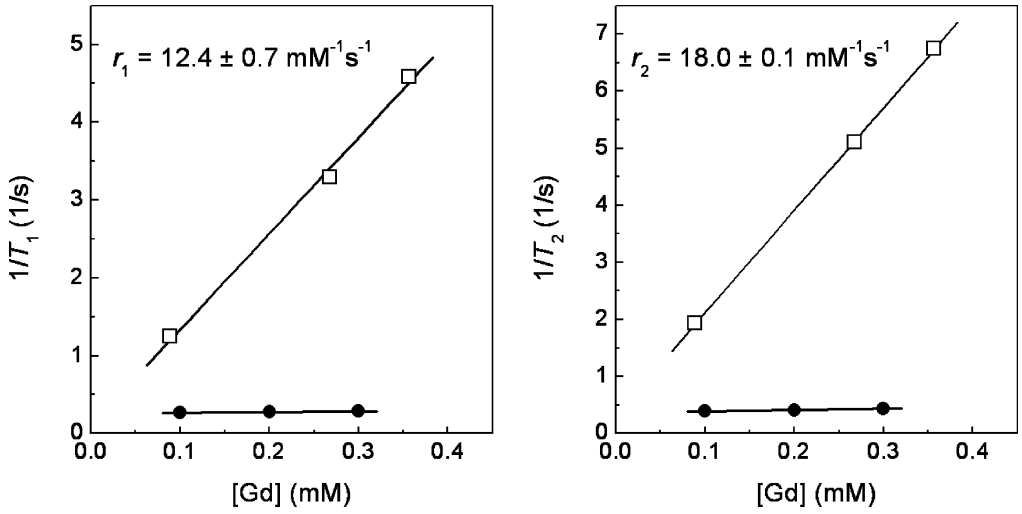

Figure 3. Longitudinal (left) and transverse (right) relaxivity of lipid-coated quantum dots with (squares) and without (circles) paramagnetic lipids in the micellular coating.

cleared by the liver less rapidly.[22] Incorporation of a large quantity of PEG lipids in a lipid mixture leads to the formation of micelles,[23] which are required for obtaining a monolayer lipid coating around the TOPO/HAD/ST capped QDs. The method used in this study has been described previously,[9] but we extended it further by incorporating magnetically labeled lipids for the simultaneous detection with magnetic resonance imaging of these water-soluable QDs. A schematic representation of this procedure is given in Figure 1. First, the lipids were dissolved in chloroform/methanol (20:1) in a 1:1 ratio. For functionalization of the QDs, 10% Mal-PEG-DSPE (1,2-distearoyl-sn-glycero-3-phosphoethanolamine-*N*-[maleimide(poly(ethylene glycol))-2000]) was added as well. The lipid mixture was added to the purified QDs in chloroform, and the solvents were evaporated gently until a dry film of lipids and QDs was obtained. Thereafter, the lipid film was heated to 70 °C and hydrated with a HEPES buffer (pH 6.7) of the same temperature. This suspension was heated and stirred vigorously until a clear suspension was obtained (Figure 2A). Empty micelles were separated from the micelles containing QDs (pQDs) by ultracentrifugation for 1 h at 500 000 g. The supernatant with empty micelles was discarded, and the pellet was suspended in HEPES buffer. The luminescence of the resulting suspension was verified by excitation with 254-nm UV light (Figure 2B). The absorption and emission spectra of the pQDs, depicted in Figure 2C, are comparable to the spectra of the original QDs in chloroform, before applying the lipid coating (see the Supporting Information).

The relaxivities, r_1 and r_2, and the potency to shorten the T_1 and T_2 relaxation time of water (and thus the potency to generate contrast in MRI) of an MRI contrast agent can be determined from the following equation

$$\frac{1}{T_{1,2,\mathrm{obs}}} = \frac{1}{T_{1,2,\mathrm{dia}}} + r_{1,2}[\mathrm{CA}]$$

which shows that the inverse of relaxation times T_1 and T_2 (i.e., $1/T_1$ and $1/T_2$) depend linearly on the contrast agent

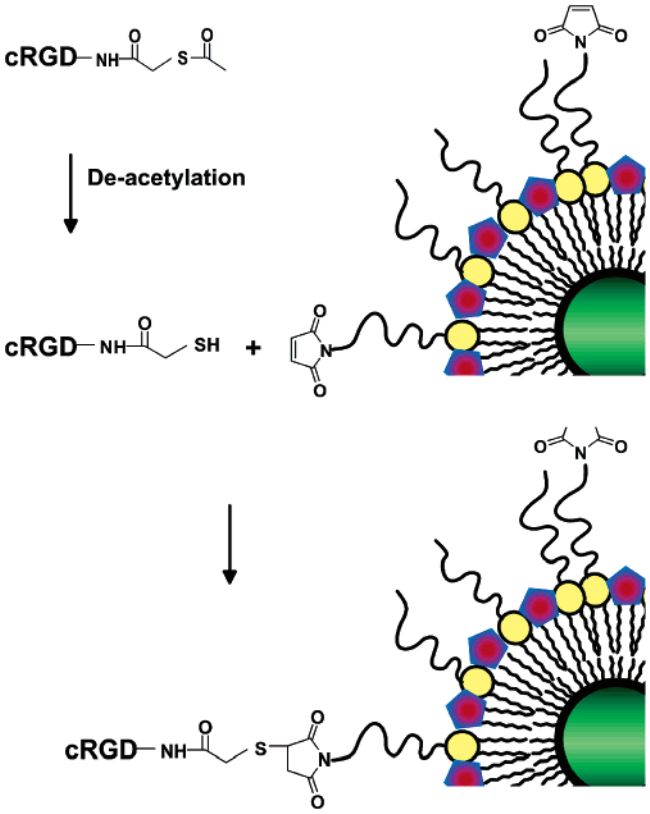

Figure 4. Schematic representation of coupling RGD to maleimide incorporated in the micellular coating after activation of the peptide.

concentration [CA] and r_1 and r_2 can be obtained by determining the slope of a plot of [CA] versus $1/T_{1,2}$. $1/T_{1,2,\mathrm{dia}}$ represents the inverse of the intrinsic T_1 or T_2, without contrast agent. Such plots, measured on a 60 MHz NMR spectrometer (Mini Spec, Bruker) are presented in Figure 3. For comparison, nonparamagnetic quantum dots (npQDs), that is, QDs without Gd-DTPA-BSA in the micellular coating, were prepared in parallel. Because the npQDs did not contain Gd, both Gd and Cd were determined with ICP to make a direct comparison of the pQDs and the npQDs possible. The ionic r_1 of the pQDs at this clinically relevant

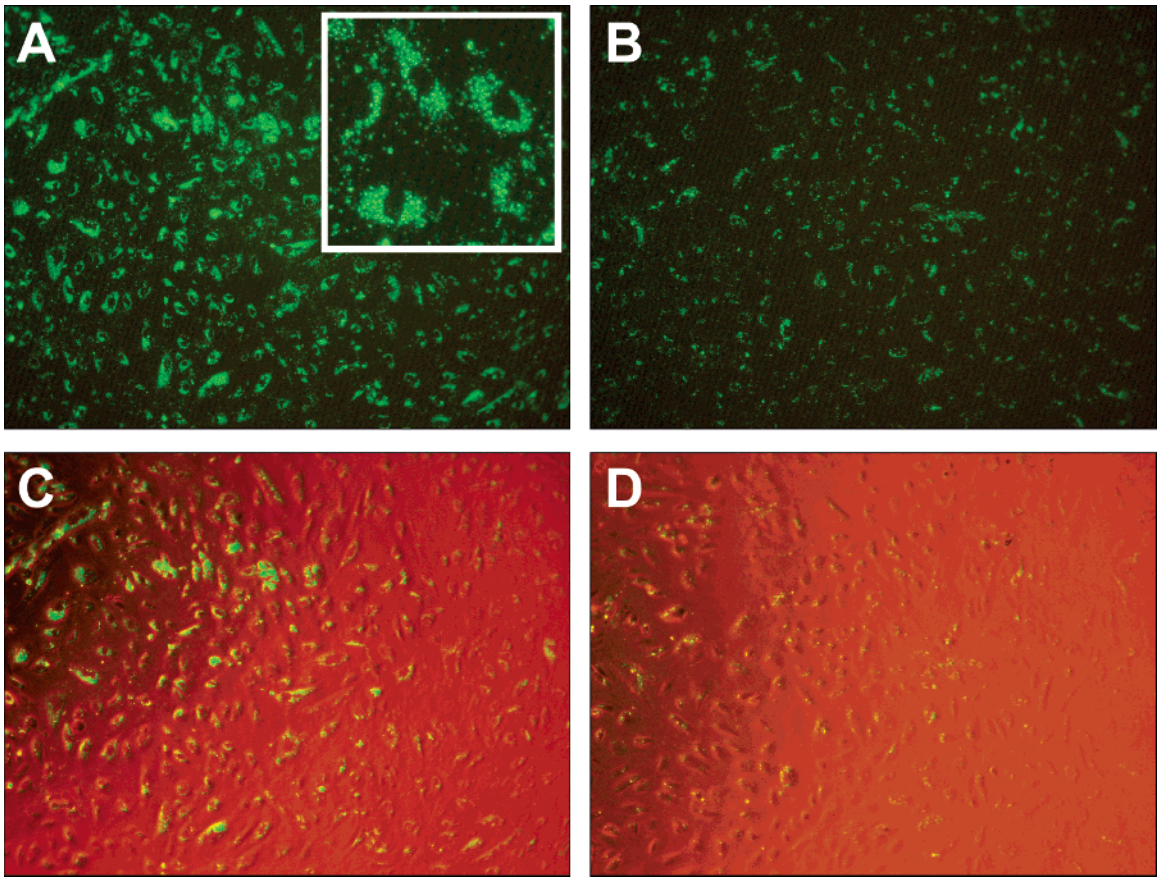

Figure 5. Fluorescence microscopy of HUVEC incubated with (A) RGD-pQDs and (B) bare pQDs. The corresponding phase contrast images of A and B are depicted in C and D, respectively.

field strength was more than 12 $mM^{-1}s^{-1}$, which is 3 times higher than that of Gd-DTPA.[3] There was hardly any effect on the relaxation rates for the npQDs with increasing concentration. Because the pQDs contain approximately 300 lipids, half of which are Gd-DTPA-BSA, the relaxivity per mM pQD was estimated to be ca. 2000 $mM^{-1}s^{-1}$. This high relaxivity makes the pQD contrast agent an attractive candidate for molecular MRI purposes.

Next, the pQDs were conjugated to cyclic RGD to make them specific for activated and angiogenic vascular endothelium. Angiogenesis, the formation of new blood vessels, is a key process in many pathological processes including cancer and atherosclerosis.[19] The identification of angiogenesis with molecular imaging methods is important for early screening and for following the effect of antiangiogenesis therapy. The conformation of the peptide sequence used in this study has been optimized for the $\alpha v\beta 3$-integrin previously.[24] It was shown that a cyclic conformation has favorable binding properties for this integrin as compared to, for example, the $\alpha v\beta 5$ integrin.[25] The cyclic 5mer RGD was synthesized with a thioacetyl group at the lysine residue for coupling. After deacetylation of the peptide, we used the thiol group to form a thioether bond between maleimide-functionalized PEG lipids, present in the micellular coat of the QDs, and cRGD (Figure 4).

Human umbilical vein endothelial cells (HUVECs) were used as an in vitro test system to assess the biological specificity of the RGD-conjugated pQDs. Proliferating HUVECs express cell surface receptors, including the $\alpha v\beta 3$-integrin, which are also expressed at angiogenic blood vessels. Therefore, RGD conjugates target to HUVEC as well and inhibit the proliferation of the cells.[26] To assess the specificity of the contrast agent, HUVECs were incubated with the $\alpha v\beta 3$-targeted pQDs (RGD-pQDs) at 37 °C. As a control, pQDs that were not conjugated with RGD were used. After, the incubation cells were washed twice. In Figure 5A, a fluorescence microscopy image of HUVECs that had been incubated with green-emitting RGD-pQDs is depicted. The RGD-pQDs were clearly associated with the cells and were found internalized at a perinuclear location (inset). Fluorescence images of HUVECs incubated with bare pQDs showed much less green fluorescence (Figure 5B). This can be explained by a nonspecific cellular uptake of the pQDs, also observed when HUVEC are incubated with liposomes.[6] Both microscopy scans were made with the same settings for laser power and photomultiplier sensitivity, allowing a direct comparison between different incubations. For clarity, the corresponding phase contrast images, which were excited with a laser simultaneously, are depicted in Figure 5C and D. The cell density for both incubations is comparable, and therefore the difference in fluorescence intensity arose from the difference in the level of association of pQDs. These results demonstrate that RGD-conjugated pQDs were actively taken up by the cells.

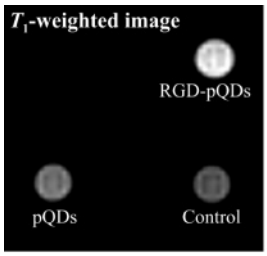

HUVEC incubated with (n=2)	T_1 (ms)	T_2 (ms)
RGD-pQDs	1123 ± 33	24.3 ± 0.3
pQDs	1673 ± 26	60.1 ± 0.6
-	1966 ± 19	87.3 ± 0.8

Figure 6. T_1-weighted image of cells that were incubated with RGD-pQDs, pQDS, or without contrast agent (left). The T_1 and T_2 relaxation times of the different cell pellets ($n = 2$) are depicted on the right.

Last, ~1.5×10^6 HUVECs were incubated with either RGD-pQDs, pQDs, or without contrast agent for 2 h at 37 °C. After the incubation, the cells were washed, put in small Eppendorf-cups, and fixed with 40 μL of 4% paraformaldehyde solution. MR imaging was performed on preparations of 1.5×10^6 packed cells. A T_1-weighted image, in which cells with a high content of Gd appear brighter than cells with a low content of Gd or no Gd, was made of cell pellets of the three incubations (Figure 6, left). The MR image of a cell pellet that was incubated with RGD-pQDs was much brighter than those that were incubated with pQDs and that were not incubated with contrast agent. Furthermore, the T_1 and T_2 relaxation times of the different cell pellets were determined (Figure 6, right). The T_1 of the pellet of HUVECs incubated with RGD-pQDs was 1123 ± 33 ms, whereas the cells incubated with pQDs had a T_1 of 1673 ± 26 ms. Cells that were not incubated with liposomes had a T_1 of 1966 ± 19 ms. The same trend was found for T_2 relaxation times (Figure 6, right). These data show that the level of association of RGD-pQDs sufficed to be detected by MRI.

Molecular imaging relies mainly on the development of potent, innovative, and specific contrast agents.[4] Intravital microscopy, for example, two photon laser scanning microscopy, is capable of visualizing multiple species at the subcellular level, but with a relatively low penetration depth and a small scanning window. QDs, in combination with intravital microscopy, have shown potential in vivo.[8,12−14] MRI is a noninvasive in vivo imaging modality capable of visualizing opaque, intact tissue at resolutions down to 50 μm.[2] Recent developments have led to more potent and more specific MRI contrast agents. This makes both imaging modalities highly complementary, and therefore the development of bimodal contrast agents, based on QDs, which can be detected with both MRI and fluorescence microscopy, may enhance the opportunities of molecular imaging greatly. Furthermore, QDs have been shown to be useful in guided surgery,[27] and recently the combination of an optical and MR detectable probe has been proposed to be useful in this field.[28]

The RGD peptide has been proven useful in drug and gene targeting in vivo[29,30] and in the field of molecular imaging. Conjugates of RGD have been used for the identification of angiogenesis with PET,[25] whereas paramagnetic perfluorcarbon nanoparticles carrying RGD mimetics[31] and paramagnetic bimodal liposomes[6] conjugated to cyclic RGD peptides[7] have shown their potential for the in vivo detection of the $\alpha v\beta 3$ integrins with MRI. Furthermore, this approach might be useful for evaluating the effect of antiangiogenesis therapy. Next to the ligand used in this study, other ligands can be conjugated to the pQDs for multimodality imaging of other markers of angiogenesis and also for imaging processes such as inflammation,[6] atherosclerosis,[32] and apoptosis.[33] The bare particle without ligand may be used to study vascular permeability with both MRI and fluorescence microscopy.[13,14,34]

In conclusion, we have shown the synthesis of quantum dots with a water-soluble and paramagnetic micellular coating as a molecular imaging probe for both fluorescence microscopy and MRI. The quantum dots preserve their optical properties and have a very high relaxivity, r_1. Targeting ligands can be coupled to these pQDs via maleimide or other functional groups. In this study, the paramagnetic quantum dots were functionalized by conjugating them with cyclic RGD peptides and were successfully targeted to human endothelial cells in vitro. We infer that this nanoparticulate bimodal contrast agent may be of great use for the detection of (tumor) angiogenesis.

Acknowledgment. We thank Professor Dr. Andries Meijerink for reading the manuscript and Dr. Holger Grüll for useful discussions. This study was financially supported by the BSIK program entitled Molecular Imaging of Ischemic Heart Disease (project no. BSIK03033).

Supporting Information Available: Materials, descriptions of the synthesis of CdSe/ZnS core/shell quantum dots, and the emission and absorption spectrum of quantum dots in chloroform. This material is available free of charge via the Internet at http://pubs.acs.org.

References

(1) Weissleder, R.; Mahmood, U. *Radiology* **2001**, *219*, 316−333.
(2) Caravan, P.; Ellison, J. J.; McMurry, T. J.; Lauffer, R. B. *Chem. Rev.* **1999**, *99*, 2293−2352.
(3) Aime, S.; Botta, M.; Fasano, M.; Terreno, E. *Chem. Soc. Rev.* **1998**, *27*, 19−29.
(4) Aime, S.; Dastru, W.; Crich, S. G.; Gianolio, E.; Mainero, V. *Biopolymers* **2002**, *66*, 419−428.
(5) Huber, M. M.; Staubli, A. B.; Kustedjo, K.; Gray, M. H.; Shih, J.; Fraser, S. E.; Jacobs, R. E.; Meade, T. J. *Bioconjugate Chem.* **1998**, *9*, 242−249.
(6) Mulder, W. J.; Strijkers, G. J.; Griffioen, A. W.; van Bloois, L.; Molema, G.; Storm, G.; Koning, G. A.; Nicolay, K. *Bioconjugate Chem.* **2004**, *15*, 799−806.
(7) Mulder, W. J.; Strijkers, G. J.; Habets, J. W.; Bleeker, J. W.; van der Schaft, D. W.; Storm, G.; Koning, G. A.; Griffioen, A. W.; Nicolay, K. *FASEB J.* **2005**.

(8) Michalet, X.; Pinaud, F. F.; Bentolila, L. A.; Tsay, J. M.; Doose, S.; Li, J. J.; Sundaresan, G.; Wu, A. M.; Gambhir, S. S.; Weiss, S. *Science* **2005**, *307*, 538−544.
(9) Dubertret, B.; Skourides, P.; Norris, D. J.; Noireaux, V.; Brivanlou, A. H.; Libchaber, A. *Science* **2002**, *298*, 1759−1762.
(10) Wu, X.; Liu, H.; Liu, J.; Haley, K. N.; Treadway, J. A.; Larson, J. P.; Ge, N.; Peale, F.; Bruchez, M. P. *Nat. Biotechnol.* **2003**, *21*, 41−46.
(11) Jaiswal, J. K.; Mattoussi, H.; Mauro, J. M.; Simon, S. M. *Nat. Biotechnol.* **2003**, *21*, 47−51.
(12) Larson, D. R.; Zipfel, W. R.; Williams, R. M.; Clark, S. W.; Bruchez, M. P.; Wise, F. W.; Webb, W. W. *Science* **2003**, *300*, 1434−1436.
(13) Gao, X.; Cui, Y.; Levenson, R. M.; Chung, L. W.; Nie, S. *Nat. Biotechnol.* **2004**, *22*, 969−976.
(14) Stroh, M.; Zimmer, J. P.; Duda, D. G.; Levchenko, T. S.; Cohen, K. S.; Brown, E. B.; Scadden, D. T.; Torchilin, V. P.; Bawendi, M. G.; Fukumura, D.; Jain, R. K. *Nat. Med.* **2005**, *11*, 678−682.
(15) Ruoslahti, E.; Pierschbacher, M. D. *Cell* **1986**, *44*, 517−518.
(16) Pedchenko, V.; Zent, R.; Hudson, B. G. *J. Biol. Chem.* **2004**, *279*, 2772−2780.
(17) Zitzmann, S.; Ehemann, V.; Schwab, M. *Cancer Res.* **2002**, *62*, 5139−5143.
(18) Pasqualini, R.; Koivunen, E.; Ruoslahti, E. *Nat. Biotechnol.* **1997**, *15*, 542−546.
(19) Griffioen, A. W.; Molema, G. *Pharmacol. Rev.* **2000**, *52*, 237−268.
(20) (a) Mekis, I.; Talapin, D. V.; Kornowski, A.; Haase, M.; Weller, H. *J. Phys. Chem. B* **2003**, *107*, 7454−7462. (b) Reiss, P.; Bleuse, J.; Pron, A. *Nano Lett.* **2002**, *2*, 781−784. (c) de Mello Donegá, C.; Hickey, S. G.; Wuister, S. F.; Vanmaekelbergh, D.; Meijerink, A. *J. Phys. Chem. B* **2003**, *107*, 489−496. (d) Steckel, J. S.; Zimmer, J. P.; Coe-Sullivan, Stott, N. E.; Bulovic, V.; Bawendi, M. G. *Angew. Chem., Int. Ed.* **2004**, *43*, 2154−2158.
(21) Fan, H.; Leve, E. W.; Scullin, C.; Gabaldon, J.; Tallant, D.; Bunge, S.; Boyle, T. *Nano. Lett.* **2005**, *5*, 645−648.
(22) Torchilin, V. P. *Nat. Rev. Drug Discovery* **2005**, *4*, 145−160.
(23) Johnsson, M.; Edwards, K. *Biophys. J.* **2003**, *85*, 3839−3847.
(24) Haubner, R.; Gratias, R.; Diefenbach, B.; Goodman, S. L.; Jonczyk, A.; Kessler, H. *J. Am. Chem. Soc.* **1996**, *118*, 7461−7472.
(25) Haubner, R.; Wester, H. J.; Weber, W. A.; Mang, C.; Ziegler, S. I.; Goodman, S. L.; Senekowitsch-Schmidtke, R.; Kessler, H.; Schwaiger, M. *Cancer Res.* **2001**, *61*, 1781−1785.
(26) Kok, R. J.; Schraa, A. J.; Bos, E. J.; Moorlag, H. E.; Asgeirsdottir, S. A.; Everts, M.; Meijer, D. K.; Molema, G. *Bioconjugate Chem.* **2002**, *13*, 128−135.
(27) Kim, S.; Lim, Y. T.; Soltesz, E. G.; De Grand, A. M.; Lee, J.; Nakayama, A.; Parker, J. A.; Mihaljevic, T.; Laurence, R. G.; Dor, D. M.; Cohn, L. H.; Bawendi, M. G.; Frangioni, J. V. *Nat. Biotechnol.* **2004**, *22*, 93−97.
(28) Veiseh, O.; Sun, C.; Gunn, J.; Kohler, N.; Gabikian, P.; Lee, D.; Bhattarai, N.; Ellenbogen, R.; Sze, R.; Hallahan, A.; Olson, J.; Zhang, M. Q. *Nano Lett.* **2005**, *5*, 1003−1008.
(29) Schiffelers, R. M.; Koning, G. A.; ten Hagen, T. L.; Fens, M. H.; Schraa, A. J.; Janssen, A. P.; Kok, R. J.; Molema, G.; Storm, G. *J. Controlled Release* **2003**, *91*, 115−122.
(30) Schiffelers, R. M.; Ansari, A.; Xu, J.; Zhou, Q.; Tang, Q.; Storm, G.; Molema, G.; Lu, P. Y.; Scaria, P. V.; Woodle, M. C. *Nucleic Acids Res.* **2004**, *32*, e149.
(31) Winter, P. M.; Caruthers, S. D.; Kassner, A.; Harris, T. D.; Chinen, L. K.; Allen, J. S.; Lacy, E. K.; Zhang, H.; Robertson, J. D.; Wickline, S. A.; Lanza, G. M. *Cancer Res.* **2003**, *63*, 5838−5843.
(32) Kelly, K. A.; Allport, J. R.; Tsourkas, A.; Shinde-Patil, V. R.; Josephson, L.; Weissleder, R. *Circ. Res.* **2005**, *96*, 327−336.
(33) van Tilborg, G. A.; Strijkers, G. J.; Mulder, W. J.; Reutelingsperger, C. P.; Nicolay, K. Proceedings of the 13th ISMRM Scientific Meeting, Miami, FL, 2005.
(34) Dafni, H.; Gilead, A.; Nevo, N.; Eilam, R.; Harmelin, A.; Neeman, M. *Magn. Reson. Med.* **2003**, *50*, 904−914.

NL051935M